JACS
JOURNAL OF THE AMERICAN CHEMICAL SOCIETY
Article
pubs.acs.org/JACS

Concentration Dependent Dimensionality of Resonance Energy Transfer in a Postsynthetically Doped Morphologically Homologous Analogue of UiO-67 MOF with a Ruthenium(II) Polypyridyl Complex

William A. Maza, Roberto Padilla, and Amanda J. Morris*

Department of Chemistry, Virginia Polytechnic Institute and State University, Blacksburg, Virginia 24061, United States

Supporting Information

ABSTRACT: A method is described here by which to dope ruthenium(II) bis(2,2′-bipyridine) (2,2′-bipyridyl-5,5′-dicarboxylic acid), RuDCBPY, into a UiO-67 metal−organic framework (MOF) derivative in which 2,2′-bipyridyl-5,5′-dicarboxylic acid, UiO-67-DCBPY, is used in place of 4,4′-biphenyldicarboxylic acid. Emission lifetime measurements of the RuDCBPY triplet metal-to-ligand charge transfer, ^{3}MLCT, excited state as a function of RuDCBPY doping concentration in UiO-67-DCBPY are discussed in light of previous results for RuDCBPY-UiO-67 doped powders in which quenching of the ^{3}MLCT was said to be due to dipole−dipole homogeneous resonance energy transfer, RET. The bulk distribution of RuDCBPY centers within MOF crystallites are also estimated with the use of confocal fluorescence microscopy. In the present case, it is assumed that the rate of RET between RuDCBPY centers has an r^{-6} separation distance dependence characteristic of Förster RET. The results suggest (1) the dimensionality in which RET occurs is dependent on the RuDCBPY concentration ranging from one-dimensional at very low concentrations up to three-dimensional at high concentration, (2) the occupancy of RuDCBPY within UiO-67-DCBPY is not uniform throughout the crystallites such that RuDCBPY densely populates the outer layers of the MOF at low concentrations, and (3) the average separation distance between RuDCBPY centers is ∼21 Å.

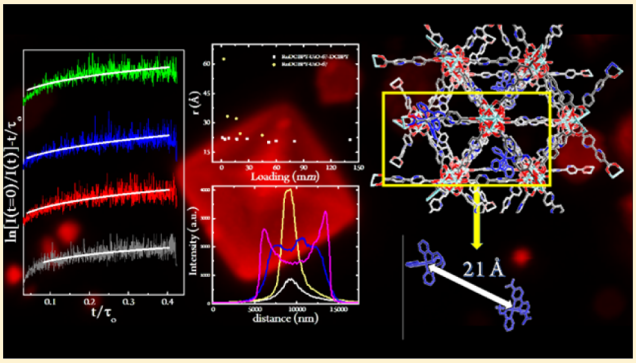

INTRODUCTION

Metal−organic frameworks (MOFs) have received a great deal of attention due to their versatility in applications. This is directly due to the tunability of their physical properties by appropriately choosing their composite ligands and metal nodes or guest molecules. The physical properties of these three-dimensional frameworks can be, and have been, further modified by postsynthetic methods.[1−3]

Recently, a great deal of interest has been spent on incorporating photoactive ligands as guest molecules in MOFs for potential photovoltaic and photocatalytic applications.[4−18] For example, a series of Re(I), Ir(III), and Ru(II) metal 5,5′-dicarboxy-2,2′-bipyridine, DCBPY, coordination complexes have been incorporated into the Zr(IV) 4,4′-biphenyldicarboxylic acid, BPDC, MOF UiO-67 for the purpose of carbon dioxide reduction, water oxidation, and organic conversion reactions.[11] The UiO-67 MOF is composed of $Zr_6(\mu_3\text{-}O)_4(\mu_3\text{-}OH)_4$ metal nodes connected by 12 BPDC ligands resulting in two distinct cavity-types: a tetrahedral cavity having a diameter of approximately 12 Å and an octahedral cavity approximately 23 Å in diameter.[19] Each of the octahedral cavities are surrounded by eight tetrahedral cavities connected by triangular windows of approximately 7 Å in height.[19−23] Together, these form a network of two-dimensional, intersecting, pyramidal channels throughout the crystal system.

Photophysical characterization of the ruthenium(II) bis(2,2′-bipyridine)(5,5′-dicarboxy-2,2′-bipyridine), RuDCBPY, doped UiO-67 as a function of doping concentration suggested the presence of two populations of ruthenium polypyridyl complexes. At low doping concentrations, the monophasic 1.4 μs emission lifetime decay was attributed to RuDCBPY incorporated into the backbone of the UiO-67 framework. At higher doping concentrations, the emission lifetime decay was nonexponential fitting best to a biexponential expression with slow and fast lifetime components on the order of 200 and 20 ns, respectively. Based on this information, it was proposed that the observed slow phase in the emission lifetime decays of the RuDCBPY-UiO-67 correspond to RuDCBPY centers incorporated into the UiO-67 backbone while the fast lifetime component was attributed to a second nonincorporated population of RuDCBPY encapsulated by the UiO-67 pores.

Confirming these claims of the RuDCBPY occupancy within UiO-67 is complicated considering that structural information regarding the majority of the UiO-*xx* and other Zr(IV)-based

Received: March 24, 2015
Published: June 4, 2015

DOI: 10.1021/jacs.5b03071
J. Am. Chem. Soc. 2015, 137, 8161−8168

Table 1. Fits of the Emission Lifetime Decays to Single Exponential Functions (τ_{obs}), the Inokuti–Hirayama Function (eq 1), and the Klafter and Blume Function (eq 4)

	loading		single exponential	Inokuti–Hirayama		Klafter and Blumen				
	m*m*	Ru/Zr_6-node	τ_{obs} (ns)	*n*	τ_o (ns)	γ	β	$d_{n=6}$	Φ_{RET}	$r_{n=6}$ (Å)[a]
RuDCBPY-UiO-67-DCBPY	1	0.031	126 ± 3	5.30	1665	2.74	0.155	0.93	0.91	22.4
	4	0.076	106 ± 7	4.37	910	2.69	0.119	0.71	0.92	21.7
	8	0.052	120 ± 3	4.92	1189	2.27	0.251	1.50	0.91	22.2
	17	0.164	106 ± 34	5.13	1352	2.44	0.262	1.57	0.92	21.7
	28	0.176	108 ± 16	5.19	1599	2.11	0.340	2.04	0.92	21.8
	52	0.380	70 ± 1	4.17	1736	2.33	0.391	2.35	0.95	20.2
	60	0.452	83 ± 10	4.27	1604	1.74	0.434	2.60	0.94	20.8
	80	0.566	78 ± 2	3.86	1706	1.82	0.380	2.28	0.94	20.6
	141	0.974	97 ± 11	5.58	2360	2.32	0.295	1.77	0.93	21.4
RuDCBPY-UiO-67[39]	2.6	0.070	1370 ± 30	3.78	1722				0.02	62.4
	6.8	0.097	720 ± 8	3.53	1750				0.49	33.3
	16.4	0.160	645 ± 6	3.25	1673				0.54	32.1
	20.6	0.187	204 ± 4	5.46	992				0.85	24.6

[a]From eq 5 using R_o = 33 Å.

frameworks has been restricted to analysis of X-ray powder diffraction patterns in combination with other diagnostic tools. These include extended X-ray fine absorption structure (EXFAS), solid state NMR, and so forth.[22,24−26] This is primarily due to the submicrometer size of the crystallites. It has been shown that the use of small molecule modulators such as acetic acid, formic acid, or benzoic acid affect the size distribution of resultant crystals within the UiO-*xx* series of MOFs leading to larger sized crystals.[27] However, data suggest that the use of these so-called modulators introduces site defects within the crystals complicating single crystal X-ray diffraction analysis.[28] It should be noted that single crystal data for UiO-66 and -67 (including functionalized derivatives thereof) have recently been obtained.[28−30] In the case of RuDCBPY-doped UiO-67, irregular nonperiodic localization of RuDCBPY throughout the framework would make resolution of structural conformation within the material difficult at best. Therefore, the conjectures proposed regarding the occupancy of UiO-67 by RuDCBPY are difficult to confirm.

Recently, a structural analogue of UiO-67 was prepared using 2,2′-bipyridine-5,5′-dicarboxylic acid in the place of 4,4′-biphenyldicarboxylic acid, UiO-67-DCBPY.[31] As a consequence, a number of reports have emerged demonstrating postsynthetic metalation of UiO-67-DCBPY by a variety of different metal salts and metal complexes.[32,33] These presumably coordinate to the DCBPY ligands of the MOF to form transition metal coordination complexes in situ incorporated directly into the backbone of the UiO-67 MOF.

This preparative scheme presented an interesting method by which to test the dual occupancy hypothesis at high doping concentrations of RuDCBPY in UiO-67. The UiO-67-DCBPY framework has been synthesized solvothermally and post-synthetically doped by incubating the material in an ethanolic solution containing ruthenium(II) bis(2,2′-bipyridine) dichloride, $Ru(bpy)_2Cl_2$. By varying the concentration of $Ru(bpy)_2Cl_2$ the concentration of RuDCBPY could then be controlled. Time-resolved emission and confocal fluorescence microscopy on the material were employed to gauge the nature of the intermolecular RuDCBPY interactions and distribution throughout the material.

MATERIALS AND METHODS

Synthesis of RuDCBPY-UiO-67-DCBPY. Undoped UiO-67-DCBPY was synthesized by suspending 130 mg of $ZrCl_4$ (0.6 mmol), 130 mg of 2,2′-bipyridine-5,5′-dicarboxylic acid (0.5 mmol), and 2.9 g of benzoic acid in a 6 dram vial containing 20 mL of dry dimethylformamide (DMF), sonicating for ∼5 min, and heating the mixture at 120 °C for 12 h. The reaction vessel and contents were allowed to cool to room temperature and filtered by washing well with DMF and EtOH. After drying, ∼100 mg of UiO-67-DCBPY was suspended in 3 mL of EtOH containing a known concentration of $Ru(bpy)_2Cl_2$, bpy = 2,2′-bipyridine. The mixture was allowed to sit at room temperature for 24 h, mixing occasionally throughout the 24 h, and then heated at 70 °C for 24 h. The resultant RuDCBPY-UiO-67-DCBPY material was filtered and washed with copious amounts of EtOH. The RuDCBPY-UiO-67-DCBPY was then soaked in fresh EtOH for 24 h, exchanging the solvent with fresh EtOH periodically to remove any unreacted $Ru(bpy)_2Cl_2$.

Powder X-ray Diffraction. X-ray powder diffraction patterns (PXRD) were obtained with a Rigaku Miniflex instrument equipped with a Cu Kα radiation source (λ = 1.5418 Å) with a 0.8°/min scan rate (0.02° step size).

Steady-State Diffuse Reflectance. Steady-state UV–visible-NIR absorption and diffuse reflectance spectra were obtained using a Cary 5000 UV–vis-NIR spectrometer. The corresponding spectra are included in the Supporting Information.

Steady-State Emission. Steady-state emission spectra were obtained using a QuantaMaster QM-200-45E (PTI) instrument equipped with a thermoelectrically cooled (Hamamatsu C9143) R2658 photomultiplier tube (PMT). Samples were excited at 450 nm with a 150 W xenon arc lamp (Ushio, UXL-151H). Samples were prepared by suspending approximately 3 mg of RuDCBPY-UiO-67-DCBPY powder in a polished four sided quartz cuvette containing ∼3 mL of DMF and a magnetic stir bar, sealed with a rubber septum and parafilm, and then purged with N_2 for 1 h. The suspensions were stirred magnetically, and the spectra were collected at a 90° relative to the incident excitation light. The spectra obtained are included in the Supporting Information.

Emission Lifetimes. Emission lifetimes were obtained by the time correlated single photon counting technique[34,35] using a QuantaMaster QM-200-45E (PTI) instrument equipped with a LED light source (510 nm, fwhm ∼ 20 nm, PTI) and PM-20 TCSPC module SPC-130. Emission lifetime decays for the magnetically stirred samples prepared by the method described above were obtained at 90° relative to the incident excitation pulse. Emission lifetime values were obtained using the DecayFit (www.fluortools.com) software package[36] by a deconvolution/reconvolution process with the instrument response

DOI: 10.1021/jacs.5b03071
J. Am. Chem. Soc. 2015, 137, 8161−8168

function (IRF). Additional scatter from the substrate/sample was accounted for in the deconvolution process.

Confocal Fluorescence Microscopy. Confocal images were collected on a Zeiss LSM 880 confocal microscope with a LED light source (excitation λ_{ex} = 488 nm), C-Apochromat 40×/1.2 W Korr FCS M27 objective, and Zen Blue (v.2) data collection and analysis software. Three dimensional imaging reconstruction was conducted in stack/time series scan mode with 0.238 μm image slice along the z-axis with 1 frame/s for 50−60 slices. Samples were suspended in water and placed in a 12-well uncoated coverglass with a thickness no. 1.5, glass diameter of 10 mm, and 18 mm in well height obtained from MatTek corporation.

Determination of RuDCBPY Loading in RuDCBPY-UiO-67-DCBPY. After postsynthetic modification, the concentration of RuDCBPY in RuDCBPY-UiO-67-DCBPY was determined by two independent methods: first by dissolving a known amount of the framework in aqueous 1 M NaOH, filtering the solution, and recording the absorption value at 450 nm. The absorption value was used in conjuction with the Beer−Lambert law to find the concentration of RuDCBPY using an exctinction coefficient of 14.6 mM^{-1} cm^{-1} for RuDCBPY at 450 nm. The concentrations obtained by this method are reported in terms of millimolal (m*m*, i.e., millimole of RuDCBPY per kilogram of MOF). Inductively coupled plasma, ICP, was also used to determine the relative number of Ru atoms per metal node of the MOF considering there are six Zr atoms per UiO-67 metal-oxo nodes. These values are reported in Table 1.

Inductively Coupled Plasma−Mass Spectrometry. Known amounts of RuDCBPY-UiO-67-DCBPY samples were digested in 70% nitric acid and heated to 90 °C for 2 h and later diluted in water so that the final concentration of nitric acid was less than 5% by volume. Samples were analyzed for ruthenium and zirconium content using a Thermo Electron X-Series inductively coupled plasma mass spectrometer (ICP-MS) in accordance with Standard Method 3125-B.

RESULTS AND DISCUSSION

X-ray powder diffraction patterns of UiO-67-DCBPY before and after RuDCBPY doping up to 141 m*m* indicate no loss of crystallinity of the sample or change in the overall structural morphology of the system (Figure 1). The ICP data indicate a linear relationship between the RuDCBPY concentrations obtained spectroscopically and the ratio of Ru to Zr_6-metal clusters (Supporting Information).

Steady-state diffuse reflectance and emission spectra indicate very little difference in the transition energies with increased doping (Figures S2 and S3 of the Supporting Information). Diffuse reflectance spectra display maxima around 450 nm consistent with a Ru($d\pi^6$)→ Ru($d\pi^5$)bpy(π^*) metal-to-ligand charge transfer transition of singlet character, ^{1}MLCT, common to ruthenium(II) tris(2,2′-bipyridine) and its derivatives.[37] The emission spectra display a maxima at ∼610 nm. The observed emission is attributed to a triplet metal-to-ligand charge transfer, ^{3}MLCT, transition commonly observed in ruthenium(II) polypyridyl coordination complexes.[38]

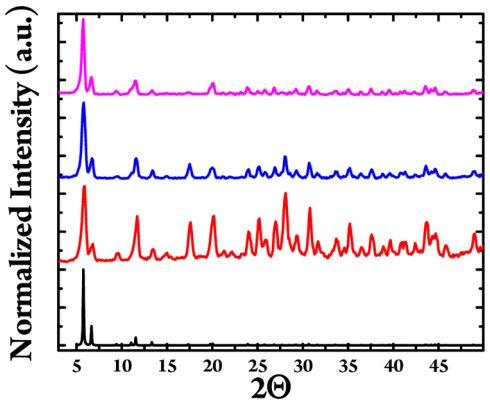

Figure 1. X-ray powder diffraction pattern of as synthesized UiO-67-DCBPY (red), RuDCBPY-UiO-67-DCBPY at doping concentrations of 4 m*m* (blue) and 141 m*m*. These are compared to the predicted pattern of UiO-67 (black).[23]

Emission lifetime decays of the RuDCBPY-doped UiO-67-DCBPY materials, RuDCBPY-UiO67-DCBPY, arising as a result of relaxation of the emissive RuDCBPY ^{3}MLCT excited state were observed to be monoexponential. Single exponential fits to the data reveal an ∼100 ns time constant at low RuDCBPY concentrations (Figure 2). The fits indicate the 100 ns RuDCBPY ^{3}MLCT is relatively insensitive to an increase in RuDCBPY doping concentration (Table 1). The ∼100 ns emission lifetimes observed here for the RuDCBPY-UiO-67-DCBPY samples at low doping concentrations differed considerably from that observed for RuDCBPY-UiO-67 (τ = 1.4 μs).[39] Interestingly, the ^{3}MLCT emission lifetimes observed for RuDCBPY-UiO-67-DCBPY do, however, resemble the slow emission lifetime component for RuDCBPY-UiO-67 at higher RuDCBPY doping concentrations (τ = ∼170 ns at 45 m*m* RuDCBPY).[39] The absence of a second, faster component to the lifetime decay is indicative of a single population of RuDCBPY throughout the material and lends legitimacy to the previous claims regarding the two observed lifetime compo-

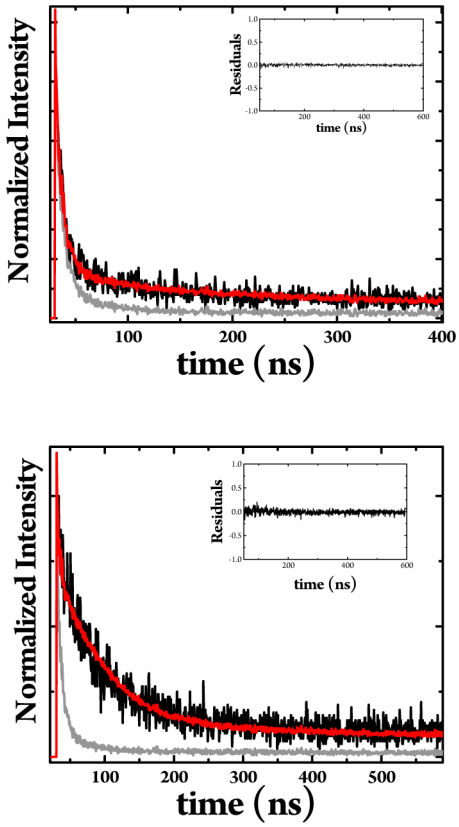

Figure 2. Time correlated single photon counting lifetime decays (black) and corresponding exponential fits (red) by a deconvolution/convolution of the instrument response function (gray) with the RuDCBPY-UiO-67-DCBPY samples at 4 m*m* (top, τ = 106 ns) and 141 m*m* (bottom, τ = 97 ns) doping concentrations. Samples were excited with a pulsed LED at 510 nm. The residuals for the fits are shown in the insets.

DOI: 10.1021/jacs.5b03071
J. Am. Chem. Soc. 2015, 137, 8161−8168

nents for RuDCBPY-doped UiO-67.[39] More specifically, the long-lifetime component of the emission lifetime of RuDCBPY-UiO-67 was attributed to RuDCBPY centers incorporated into the UiO-67 backbone whereas the fast lifetime component was attributed to encapsulated RuDCBPY centers.

The large decrease in the RuDCBPY ^{3}MLCT lifetime observed previously upon increasing the RuDCBPY concentration in RuDCBPY-UiO-67 was attributed to homogeneous resonance energy transfer, RET, between RuDCBPY centers within the framework of the material.[39] The emission lifetime data was fit to the Inokuti–Hirayama function:[40,41]

$$I(t) = I(t=0)\exp\left[-\frac{t}{\tau_o} - \Gamma\left(1-\frac{3}{n}\right)\left(\frac{C_A}{C_o}\right)\left(\frac{t}{\tau_o}\right)^{3/n}\right] \quad (1)$$

which is a generalized expression describing the effect of the donor emission lifetime (τ_o) on the acceptor concentration (C_A) and a distance dependent empirical term n. In the equation above, $I(t = 0)$ is the emission intensity immediately after excitation and C_o is the critical concentration at which the probability of RET is 50%. The distance dependence term, n, takes on the values n = 6, 8, and 10 for dipole–dipole, dipole–quadrupole, and quadrupole–quadrupole interactions, respectively.[40−42] In the case that n = 6, eq 1 reduces to the familiar form of Förster-type energy transfer, FRET:

$$I(t) = I(t=0)\exp\left[-\frac{t}{\tau_o} - 2\left(\frac{C_A}{C_o}\right)\left(\frac{t}{\tau_o}\right)^{1/2}\right] \quad (2)$$

If n = 3, however, then eq 1 becomes exponential indicating either an exchange mechanism of RET (i.e., Dexter-type energy transfer, DRET), or Perrin-type excitonic energy transfer (i.e., weak or strong coupling).

The RuDCBPY-UiO-67-DCBPY emission lifetime decays were fit to eq 1, and the results summarized in Table 1. The emission lifetime values obtained from deconvolution analyses using the instrument response function and a single exponential decay model are also shown in Table 1. The C_o, n, and τ_o parameters were allowed to vary while fixing C_A to the doping concentration. The values obtained for τ, n, C_o, and τ_o were found to be invariant with increasing RuDCBPY concentration. On average, the τ, n, C_o, and τ_o were 99 ± 19 ns, 4.32 ± 1.4, 20.9 ± 18.8 mm, and 1680 ± 531 ns, respectively. These agree well with results obtained previously for RuDCBPY-UiO-67.[39]

The fits to eq 1 obtained from the emission lifetime decays for the RuDCBPY-UiO-67-DCBPY samples suggest an r^{-4} distance dependence on the rate of dipole–dipole RET between RuDCBPY centers. Similarly, the results obtained from the fits to eq 1 to the RuDCBPY-UiO-67 data reported by Maza and Morris also indicated an r^{-4} distance dependence for RET between RuDCBPY centers.[39] From this, it was argued that the degree of coupling between RuDCBPY centers lie somewhere between the very weak (Förster) coupling regime and the weak (Perrin or Dexter) regime.[39] It was pointed out that some speculation exists regarding a continuum existing along the coupling coordinate of the distance dependence on RET despite the lack of a unifying theory linking the very weak, weak and strong coupling regimes on the coordinate.[43] In the majority of the cases, this r^{-4} dependent mechanism of electronic energy transfer occurs between molecular excited states and the surfaces of metals and metal nanoparticles.[44]

That said, an r^{-4} distance dependence on the rate of energy transfer here suggests that quenching of the RuDCBPY ^{3}MLCT is brought about by interaction with the $Zr_6O_4(OH)_4(COO)_{12}$ nodes of the UiO-67/UiO-67-DCBPY. However, this does not explain the observed effect of increased RuDCBPY-doping on the RuDCBPY ^{3}MLCT lifetime. If the origin of the lifetime quenching is, indeed, an interaction between the RuDCBPY ^{3}MLCT and the $Zr_6O_4(OH)_4(COO)_{12}$ nodes, one would expect the observed emission lifetime to depend on the concentration of $Zr_6O_4(OH)_4(COO)_{12}$ relative to RuDCBPY concentration. This would result and an increase in the observed RuDCBPY emission lifetime with an increase in doping concentration.

This r^{-4} dependence is based on the assumption that the distribution of RuDCBPY centers in both RuDCBPY-UiO-67 and RuDCBPY-UiO-67-DCBPY is random and uniform throughout the MOF and that the resulting RET occurs in three dimensions about the energy donor. The system can, however, be treated more generally using a different approach, developed by Klafter and Blumen, if the distribution of RuDCBPY doping of UiO-67-DCBPY as fractal-like.[45] That is, it is possible that the distribution of RuDCBPY in UiO-67 and UiO-67-DCBPY is irregular resulting in isolated regions of densely populated RuDCBPY throughout the framework of the MOF. As a consequence, the rate of energy transfer would not be dependent on the regular dimension of the MOF, d, but rather on the fractal dimension, đ.

For FRET, however, the fractal dimension đ ≈ d. Equation 1, then, takes the form:[45−48]

$$I(t) = I(t=0)\exp\left[-\frac{t}{\tau_o} - \gamma\Gamma(1-\beta)\left(\frac{t}{\tau_o}\right)^{\beta}\right] \quad (3a)$$

where

$$\beta = \frac{d}{n} \quad (3b)$$

In eq 3, $\Gamma(t)$ is the gamma function

$$\Gamma(t) = \int_0^\infty x^{t-1}\, e^{-x}\, dx \quad (3c)$$

and γ is related to the relative occupancy and positions of the donor and acceptors within the fractal space. For three-dimensional Förster-type energy transfer (d = 3, n = 6), $\gamma = C_A/C_o$, where C_A is the actual acceptor concentration. The term C_o is the critical acceptor concentration at which the probability of energy transfer is 50% defined by Förster as $C_o = 3/(4\pi^{3/2}R_o^3)$ where R_o is the critical transfer distance. In two dimensions (d = 2, n = 6), γ, C_A, and C_o have the same meaning where $C_o = 6/(\pi R_o^2)$.[49] In terms of the fractal dimension, đ,

$$\gamma = x_a(d/đ)V_d R_o^{đ}\Gamma(1-\beta) \quad (3d)$$

where V_d is the volume of the donor quenching sphere with dimension d, and x_a is the fraction of populated fractal sites.

Equation 3 can be rearranged to yield

$$\ln\left[\frac{I(t=0)}{I(t)}\right] - \frac{t}{\tau_o} = \gamma\Gamma(1-\beta)\left(\frac{t}{\tau_o}\right)^{\beta} \quad (4)$$

By fitting the RuDCBPY ^{3}MLCT emission lifetime decays to eq 4 (Figure 3), it was found that γ was invariant to changes in RuDCBPY doping. In contrast, β was observed to increase from

DOI: 10.1021/jacs.5b03071
J. Am. Chem. Soc. 2015, 137, 8161−8168

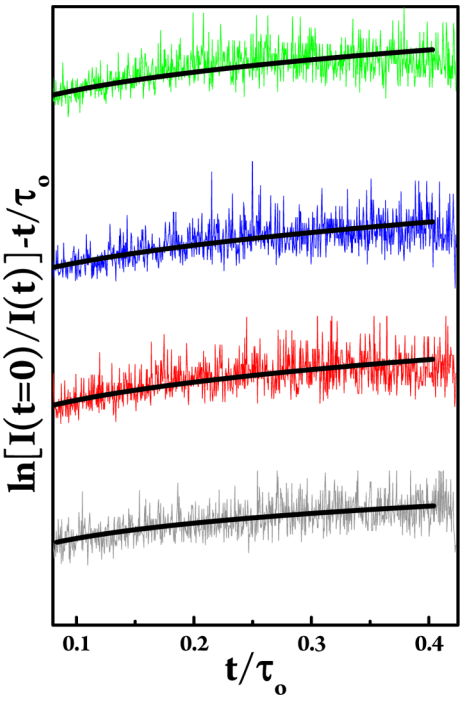

Figure 3. Klafter–Blumen plots for RuDCBPY-UiO-67-DCBPY ^{3}MLCT emission lifetime decays at 8 m*m* (gray), 28 m*m* (red), 60 m*m* (blue), and 141 m*m* (green). The solid black lines represent best fits to the data using eq 4.

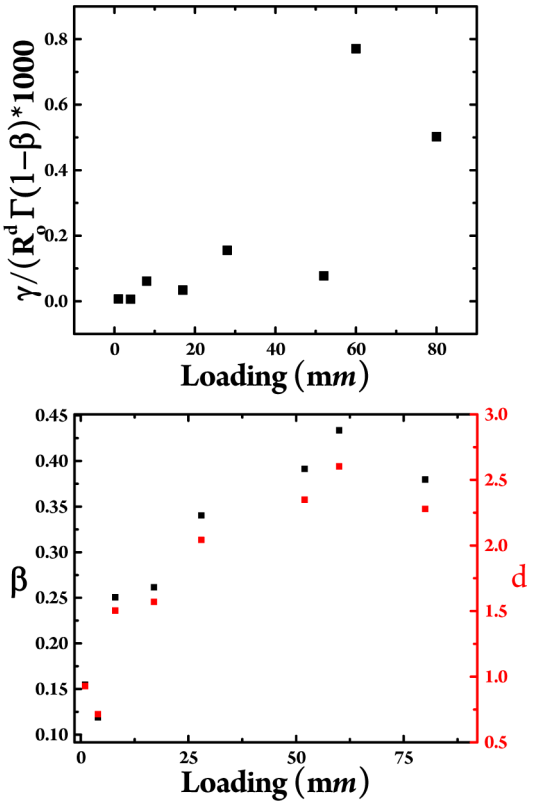

Figure 4. Overlay of the β and resulting đ values (top) as well as the γ values (bottom) obtained from the fits to eq 4 as a function of postsynthetic RuDCBPY-loading concentration in UiO-67-DCBPY.

$\beta \approx 0.2$ at low RuDCBPY concentrations to $\beta \approx 0.4$ at higher RuDCBPY concentrations (Table 1, Figure 4). If $n = 6$, then the dimensional factor d ranges between ~1 and approaches 3 with increased RuDCBPY loading. The average value of β within the concentration range used was 0.29 ± 0.11. Assuming a Förster-type dipole–dipole interaction ($n = 6$), an average value of 1.74 ± 0.64 was obtained for d over the concentration range used, suggesting a two-dimensional RET mechanism.

It should be noted that one- and two-dimensional RET has been observed between energy donors and acceptors associated with a number of different materials having restricted geometries.[34,50−54] In particular, two-dimensional RET is quite common between interacting energy donors and acceptors adsorbed on surfaces.[34,51,53,55−57] Additionally, Minkowski and Clazaferri have observed two-dimensional RET between donor and acceptor chromophores doped within the channels of mesoporous zeolite L.[58]

Interestingly, similar values for đ (đ = 1.74 ± 0.12) have been found for RET between rhodamine B and malachite green adsorbed into the pores of Vycor 7930 glass.[59] Fluorescence lifetime quenching of rhodamine B (RB) or rhodamine 6G (R6G) energy donors by malachite green (MG) acceptors on the surface of polystyrene latex also show a đ ~ 1.8, whereas RB-MG and R6G-MG display a đ ~ 2.0 on poly(butyl methacrylate) surfaces.[51,56] In the case of dioctadecylpyronine (PYR18, donor) and dioctadecyl crystal violet (CV18, acceptor) adsorbed onto Langmuir–Blodgett films, the value obtained for đ from fluorescence lifetime fits were found to increase from đ = 2.0 to đ = 3.0 upon stacking additional Langmuir–Blodgett film layers and increasing the concentration of CV18.

It is observed here that β and, more importantly, đ (assuming very-weak coupling between the donor and acceptor transition dipoles) both increase when the concentration of RuDCBPY is increased in UiO-67-DCBPY. The variation of đ with RuDCBPY doping explains the relative invariability of γ over the concentration range (vide supra). Interestingly, the values found for đ appear to be ~1 at low concentrations, and quickly approach 3 as the number of RuDCBPY centers in UiO-67-DCBPY increase. The average intermolecular distance between interacting RuDCBPY centers, r, can be estimated from[60]

$$\Phi_{RET} = 1 - \frac{\tau}{\tau_o} = \frac{1}{1 + (r/R_o)^n} \quad (5)$$

If, indeed, the distance dependence of k_{RET} is on the order of r^{-6} (contrary to what is obtained using eq 1 where đ is assumed to be 3), then, like γ, r is relatively invariant in the concentration range probed and is 21.4 ± 0.8 Å on average where R_o is taken to be ~33 Å (Figure 5).[39]

The trends observed here for đ, together with the r values calculated from eq 5 are suggestive of a few interesting results if the dipole–dipole interactions between RuDCBPY are indeed of the Förster-type where $n = 6$. First, the variation in đ is indicative of a concentration dependence on the dimensionality of RET where at low concentrations of RuDCBPY (<10 m*m*) RET is one-dimensional, then two-dimensional at concentrations between ~10 and ~50 m*m* above which a percolation limit is met resulting in three-dimensional RET. Second, the relative invariability of the intermolecular separation between RuDCBPY centers suggest that RuDCBPY doping in UiO-67-DCBPY by this postsynthetic method is nonuniform resulting in erratic clusters of dense RuDCBPY populations throughout the material.

Emission microscopy data was collected along the z-axis (relative to the laboratory/microscope coordinate plane) of

DOI: 10.1021/jacs.5b03071
J. Am. Chem. Soc. 2015, 137, 8161−8168

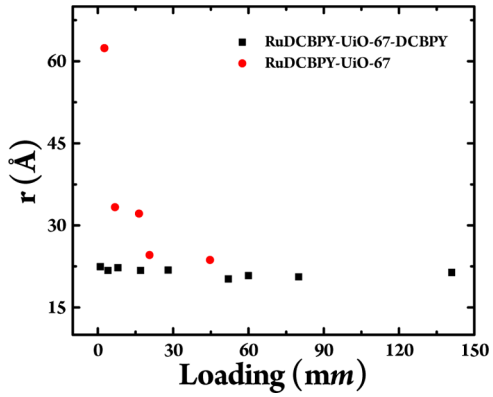

Figure 5. Calculated average intermolecular donor−acceptor distances, *r*, at each concentration of RuDCBPY-doped into UiO-67-DCBPY (black squares) compared to the results obtained by Maza and Morris[39] for RuDCBPY-UiO-67 (red circles).

IRMOF-10 crystals into which was diffused ruthenium(II) bis(2,2′-bipyridine) (2,2′-bipyridyl-4,4′-diphosphonate), RuDPBPY, at varying concentrations.[61] It was observed that, at lower concentrations, the RuDPBPY doping is inhomogeneous throughout the crystal system—restricted to the outermost layers of the crystal. At higher RuDPBPY concentrations, however, the RuDPBPY dopant penetrates further into the crystal populating more of the interior reaching a saturating concentration limit where the crystal is nearly uniformly doped.

A similar fluorescence microscopy analysis was performed here on RuDCBPY-UiO-67-DCBPY samples doped at 4, 28, and 141 m*m*. In much the same way as RuDPBPY doping in IRMOF-10, it was expected that doping RuDCBPY within UiO-67-DCBPY by diffusion of $Ru(bpy)_2$ into the MOF and heating would form densely packed RuDCBPY centers at the outer layers of the MOF at low concentrations, populating more of the inner layers with increased $Ru(bpy)_2$ concentration in the postsynthetic doping procedure. At all doping concentrations probed, scans taken along the *z*-axis indicate a multimodal distribution of emission intensity along the width of the crystal upon approach to the center of the crystal height (Figure 6). A three-dimensional rendering of the emission data from the *z*-scans indicates that these bands correspond to regions of increased RuDCBPY density along the edges of the crystal (Figure 7; see also the movie in the Supporting Information). Considerably less intensity, however, was observed within the internal area of the slices indicating reduced RuDCBPY population in this region. In addition, the multiple bands observed along the middle of the crystal were observed to collapse into a single band as the focal point of the excitation approached a crystal vertex.

The results are interesting in that they suggest a large density of RuDCBPY near, or on, the surface of UiO-67-DCBPY, particularly along the vertices and edges of the crystal. Despite that, the center of the crystallites observed are not entirely devoid of RuDCBPY centers as evidenced from the spatial intensity profiles shown in Figure 6. Cursory modeling of possible RuDCBPY occupancies in the UiO-67 and UiO-67-DCBPY frameworks indicate that interactions between RuDCBPY centers may occur between RuDCBPY located in adjacent octahedral and tetrahedral pores. These observations, coupled to the fits of the data obtained from eq 4, imply that the population of RuDCBPY along the edges and vertices dominate the observed emission. The intermolecular interactions between the RuDCBPY centers along these regions resemble two-dimensional FRET observed on surfaces of membranes and other surfaces suggesting these interactions occur between RuDCBPY located on the surface of the MOF.[34] If so, the diffusion gradients of $Ru(bpy)_2$ populating the pores of UiO-67-DCBPY during the postsynthetic procedure may originate at the edges and vertices of MOF crystallites. As the saturation concentration is approached, in which the interior layers of the MOF crystallites become more evenly doped, the FRET mechanism becomes three-dimensional in nature.

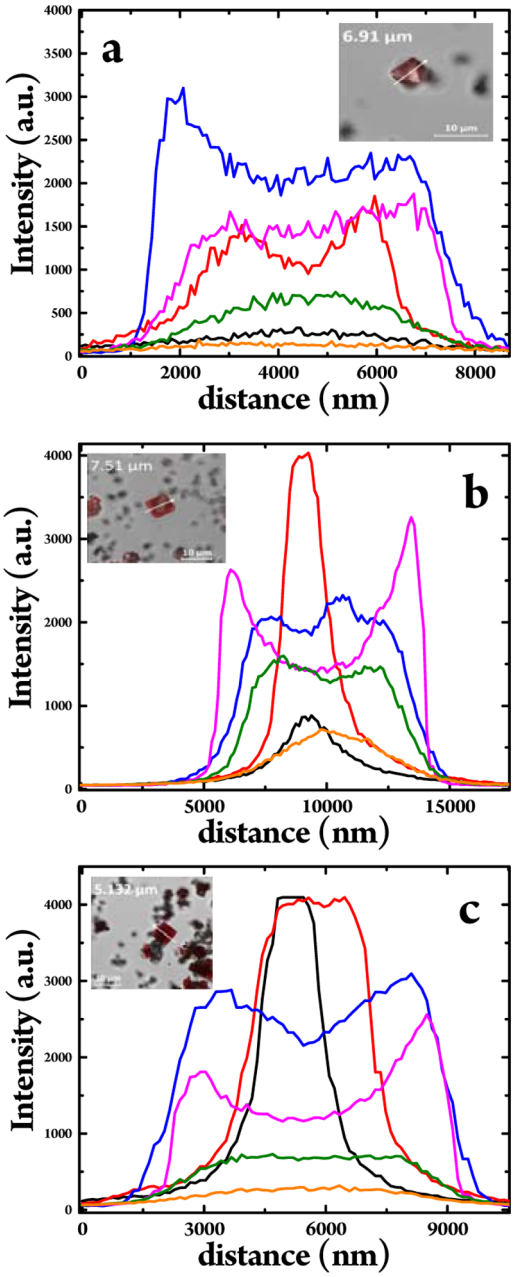

Figure 6. Spatial emission intensity profiles obtained by confocal emission microscopy of (a) 4 m*m*, (b) 28 m*m*, and (c) 141 m*m* RuDCBPY-UiO-67-DCBPY samples suspended in water as a function of incident excitation focal point position along the *z*-axis: (black) ∼1 μm, (red) 2 μm, (blue) 4 μm, (pink) 7 μm, (green) 10 μm, and (orange) 13 μm from $z = 0$ μm position of the *z*-scan. Insets show the one-dimensional axis (white arrow) along the crystals corresponding to the data shown.

DOI: 10.1021/jacs.5b03071
J. Am. Chem. Soc. 2015, 137, 8161−8168

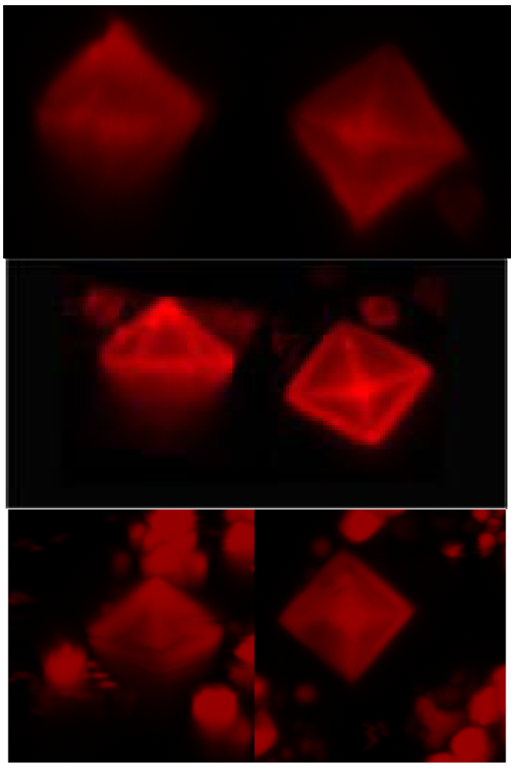

Figure 7. Three-dimensional renderings of confocal fluorescence microscopy images taken for single RuDCBPY-UiO-67-DCBPY crystals doped at (top) 4m*m*, (middle) 28 m*m*, and (bottom) 141 m*m* as viewed from the side (left) and from the top (right).

During the course of this work, a number of reports have been made available describing postsynthetic modifications of UiO-type MOFs.[32,33] In particular, this same UiO-67-DCBPY has been modified to contain transition metal DCBPY complex sites along the backbone of the MOF by Long et al. by diffusion of transition metal salts into the material with gentle heating.[33] Single crystal X-ray diffractions of the doped MOFs displayed crystallographically resolvable M(DCBPY) centers (M = $CuCl_2$, CuCl, $CoCl_2$, $FeBr_2$, and $Cr(CO)_4$) where coordination of the metal salt resulted in decreased symmetry of the crystal system. The report also describes postsynthetic incorporation of the molecular catalyst $Ir(COD)BF_4$, COD = 1,5-cyclooctadiene; however, single crystal analysis indicated less than 10% occupancy of the DCBPY sites which were poorly resolved crystallographically.

The results obtained here for the postsynthetic doping of UiO-67-DCBPY with $Ru(bpy)_2$ may offer broader insight into other transition metal complexes doped into UiO-67-DCBPY. A quantitative structure−activity relationship, QSAR, calculation of the van der Waals volume of $Ru(bpy)_2Cl_2$ indicates a diameter of ∼10 Å of the bis-chelate based on a hard spheres approximation.[39] The calculated radius of the dopant should not be a limitation to penetration into the bulk of UiO-67-DCBPY given the ∼7 Å height of the triangular windows (vida supra). Despite this, it is evident from the microscopy data that free diffusion of $Ru(bpy)_2Cl_2$ into the bulk of the material is hindered in some way. It is possible that the same mechanism of diffusion of $Ru(bpy)_2Cl_2$ may govern the irregular doping of UiO-67-DCBPY by $Ir(COD)BF_4$ and other transition metal complexes, limiting the extent and uniformity of postsynthetic MOF doping.

CONCLUSIONS

A postsynthetic method of doping the UiO-67 metal−organic framework, MOF, with the photoactive metal polypyridyl complex, ruthenium(II) bis(2,2′-bipyridine) (2,2′-bipyridyl-4,4′-dicarboxylic acid), RuDCBPY, has been described. Its occupancy of the framework and excited state deactivation is discussed based on the RuDCBPY triplet metal-to-ligand (^{3}MLCT) excited state emission lifetime at different doping concentrations. It is argued that when UiO-67-DCBPY is saturated with RuDCBPY, the quenched ^{3}MLCT lifetime is due to Förster-type dipole−dipole homogeneous three-dimensional resonance energy transfer between RuDCBPY centers located throughout the material at separation distances of ∼21 Å. At low doping concentrations, however, doping of the MOF is irregular where the innermost interior layers of the MOF remain less populated compared to outermost layers or, more specifically, the vertices and edges of the crystallites. At these low concentrations, a two-dimensional mechanism of FRET is thought to dominate the self-quenching reaction of RuDCBPY, implying a prevalence of surface bound intermolecular interactions between RuDCBPY centers.

ASSOCIATED CONTENT

Supporting Information

Comparison of X-ray powder diffraction patterns, steady-state diffuse reflectance, steady-state emission, and goodness of fit and residuals of the lifetime deconvolutions; surface area analysis of the RuDCBPY-UiO-67-DCBPY crystals at 4 m*m*; movie (in avi format) showing a three-dimensional rendering of the emission data. The Supporting Information is available free of charge on the ACS Publications website at DOI: 10.1021/jacs.5b03071.

AUTHOR INFORMATION

Corresponding Author

*ajmorris@vt.edu

Notes

The authors declare no competing financial interest.

ACKNOWLEDGMENTS

The authors would like to thank Jeffrey L. Parks for providing the ICP data. This material is based upon work supported by the U.S. department of Energy, Office of Basic Energy Sciences under Award Number DE-SC0012446.

REFERENCES

(1) Kandiah, M.; Usseglio, S.; Svelle, S.; Olsbye, U.; Lillerud, K. P.; Tilset, M. *J. Mater. Chem.* **2010**, *20*, 9848−9851.
(2) Banerjee, M.; Das, S.; Yoon, M.; Choi, H. J.; Hyun, M. H.; Park, S. M.; Seo, G.; Kim, K. *J. Am. Chem. Soc.* **2009**, *131*, 7524−7525.
(3) Burrows, A. D.; Frost, C. G.; Mahon, M. F.; Richardson, C. *Angew. Chem., Int. Ed.* **2008**, *47*, 8482−8486.
(4) Larsen, R. W.; Miksovska, J.; Musselman, R. L.; Wojtas, L. *J. Phys. Chem. A* **2011**, *115*, 11519−11524.
(5) Larsen, R. W.; Wojtas, L. *J. Phys. Chem. A* **2012**, *116*, 7830−7835.
(6) Kent, C. A.; Liu, D.; Meyer, T. J.; Lin, W. *J. Am. Chem. Soc.* **2012**, *134*, 3991−3994.
(7) Kent, C. A.; Liu, D. M.; Ito, A.; Zhang, T.; Brennaman, M. K.; Meyer, T. J.; Lin, W. B. *J. Mater. Chem. A* **2013**, *1*, 14982−14989.
(8) Kent, C. A.; Liu, D. M.; Ma, L. Q.; Papanikolas, J. M.; Meyer, T. J.; Lin, W. B. *J. Am. Chem. Soc.* **2011**, *133*, 12940−12943.
(9) Kent, C. A.; Mehl, B. P.; Ma, L. Q.; Papanikolas, J. M.; Meyer, T. J.; Lin, W. B. *J. Am. Chem. Soc.* **2010**, *132*, 12767−12769.

DOI: 10.1021/jacs.5b03071
J. Am. Chem. Soc. 2015, 137, 8161−8168

(10) Lin, J. X.; Hu, X. Q.; Zhang, P.; Van Rynbach, A.; Beratan, D. N.; Kent, C. A.; Mehl, B. P.; Papanikolas, J. M.; Meyer, T. J.; Lin, W. B.; Skourtis, S. S.; Constantinou, M. *J. Phys. Chem. C* **2013**, *117*, 22250−22259.
(11) Wang, C.; Xie, Z.; deKrafft, K. E.; Lin, W. *J. Am. Chem. Soc.* **2011**, *133*, 13445−13454.
(12) So, M. C.; Wiederrecht, G. P.; Mondloch, J. E.; Hupp, J. T.; Farha, O. K. *Chem. Commun.* **2015**, 3501−3510.
(13) Lee, D. Y.; Shin, C. Y.; Yoon, S. J.; Lee, H. Y.; Lee, W.; Shrestha, N. K.; Lee, J. K.; Han, S. H. *Sci. Rep.* **2014**, *4*, 3930−3935.
(14) Foster, M. E.; Azoulay, J. D.; Wong, B. M.; Allendorf, M. D. *Chem. Sci.* **2014**, *5*, 2081−2090.
(15) Williams, D. E.; Rietman, J. A.; Maier, J. M.; Tan, R.; Greytak, A. B.; Smith, M. D.; Krause, J. A.; Shustova, N. B. *J. Am. Chem. Soc.* **2014**, *136*, 11886−11889.
(16) Whittington, C. L.; Wojtas, L.; Larsen, R. W. *Inorg. Chem.* **2014**, *53*, 160−166.
(17) Whittington, C. L.; Wojtas, L.; Gao, W.-Y.; Ma, S.; Larsen, R. W. *Dalton Trans.* **2015**, *44*, 5331−5337.
(18) Chambers, M. B.; Wang, X.; Elgrishi, N.; Hendon, C. H.; Walsh, A.; Bonnefoy, J.; Canivet, J.; Quadrelli, E. A.; Farrusseng, D.; Mellot-Draznieks, C.; Fontecave, M. *ChemSusChem* **2015**, *8*, 603−608.
(19) Bon, V.; Senkovska, I.; Weiss, M. S.; Kaskel, S. *CrystEngComm* **2013**, *15*, 9572−9577.
(20) DeCoste, J. B.; Peterson, G. W.; Jasuja, H.; Glover, T. G.; Huang, Y. G.; Walton, K. S. *J. Mater. Chem. A* **2013**, *1*, 5642−5650.
(21) Katz, M. J.; Brown, Z. J.; Colon, Y. J.; Siu, P. W.; Scheidt, K. A.; Snurr, R. Q.; Hupp, J. T.; Farha, O. K. *Chem. Commun.* **2013**, *49*, 9449−9451.
(22) Cavka, J. H.; Jakobsen, S.; Olsbye, U.; Guillou, N.; Lamberti, C.; Bordiga, S.; Lillerud, K. P. *J. Am. Chem. Soc.* **2008**, *130*, 13850−13851.
(23) Yang, Q. Y.; Guillerm, V.; Ragon, F.; Wiersum, A. D.; Llewellyn, P. L.; Zhong, C. L.; Devic, T.; Serre, C.; Maurin, G. *Chem. Commun.* **2012**, *48*, 9831−9833.
(24) Chavan, S.; Vitillo, J. G.; Gianolio, D.; Zavorotynska, O.; Civalleri, B.; Jakobsen, S.; Nilsen, M. H.; Valenzano, L.; Lamberti, C.; Lillerud, K. P.; Bordiga, S. *Phys. Chem. Chem. Phys.* **2012**, *14*, 1614−1626.
(25) Valenzano, L.; Civalleri, B.; Chavan, S.; Bordiga, S.; Nilsen, M. H.; Jakobsen, S.; Lillerud, K. P.; Lamberti, C. *Chem. Mater.* **2011**, *23*, 1700−1718.
(26) Gianolio, D.; Vitillo, J. G.; Civalleri, B.; Bordiga, S.; Olsbye, U.; Lillerud, K. P.; Valenzano, L.; Lamberti, C. *J. Phys. Conf. Ser.* **2013**, *430*, 012134−012140.
(27) Schaate, A.; Roy, P.; Godt, A.; Lippke, J.; Waltz, F.; Wiebcke, M.; Behrens, P. *Chem.—Eur. J.* **2011**, *17*, 6643−6651.
(28) Oien, S.; Wragg, D.; Reinsch, H.; Svelle, S.; Bordiga, S.; Lamberti, C.; Lillerud, K. P. *Cryst. Growth. Des.* **2014**, *14*, 5370−5372.
(29) Ko, N.; Hong, J.; Sung, S.; Cordova, K. E.; Park, H. J.; Yang, K.; Kim, J. *Dalton Trans.* **2015**, *44*, 2047−2051.
(30) Furukawa, H.; Gandara, F.; Zhang, Y. B.; Jiang, J. C.; Queen, W. L.; Hudson, M. R.; Yaghi, O. M. *J. Am. Chem. Soc.* **2014**, *136*, 4369−4381.
(31) Li, L.; Tang, S.; Wang, C.; Lv, X.; Jiang, M.; Wu, H.; Zhao, X. *Chem. Commun.* **2014**, *50*, 2304−2307.
(32) Manna, K.; Zhang, T.; Lin, W. B. *J. Am. Chem. Soc.* **2014**, *136*, 6566−6569.
(33) Gonzalez, M. I.; Bloch, E. D.; Mason, J. A.; Teat, S. J.; Long, J. R. *Inorg. Chem.* **2015**, *54*, 2995−3005.
(34) Valeur, B.; Berberan-Santos, M. N. *Molecular fluorescence principles and applications*, 2nd ed.; Wiley: Weinheim, 2012.
(35) O'Connor, D. *Time-correlated single photon counting*; Academic Press: London, 1984.
(36) Yang, R. T. *Gas Separation By Adsorption Processes*; Butterworth: Boston, 1987.
(37) Juris, A.; Campagna, S.; Balzani, V.; Gremaud, G.; Vonzelewsky, A. *Inorg. Chem.* **1988**, *27*, 3652−3655.
(38) Juris, A.; Balzani, V.; Barigelletti, F.; Campagna, S.; Belser, P.; Vonzelewsky, A. *Coord. Chem. Rev.* **1988**, *84*, 85−277.
(39) Maza, W. A.; Morris, A. J. *J. Phys. Chem. C* **2014**, *118*, 8803−8817.
(40) Inokuti, M.; Hirayama, F. *J. Chem. Phys.* **1965**, *43*, 1978−1989.
(41) Kellogg, R. E. *J. Chem. Phys.* **1967**, *47*, 3403−3406.
(42) Berberan-Santos, M. N.; Bodunov, E. N.; Valeur, B. *Chem. Phys.* **2005**, *317*, 57−62.
(43) Kenkre, V. M.; Knox, R. S. *Phys. Rev. Lett.* **1974**, *33*, 803−806.
(44) Rogach, A. L.; Klar, T. A.; Lupton, J. M.; Meijerink, A.; Feldmann, J. *J. Mater. Chem.* **2009**, *19*, 1208−1221.
(45) Klafter, J.; Blumen, A. *J. Chem. Phys.* **1984**, *80*, 875−877.
(46) Klafter, J.; Blumen, A.; Zumofen, G. *J. Stat. Phys.* **1984**, *36*, 561−577.
(47) Klafter, J.; Blumen, A.; Zumofen, G. *J. Lumin.* **1984**, *31*−*2*, 627−633.
(48) Klafter, J.; Blumen, A. *J. Chem. Phys.* **1984**, *80*, 875−877.
(49) Rolinski, O. J.; Birch, D. J. S.; McCartney, L. J.; Pickup, J. C. *Chem. Phys. Lett.* **1999**, *309*, 395−401.
(50) Webber, S. E. *Chem. Rev.* **1990**, *90*, 1469−1482.
(51) Nakashima, K.; Duhamel, J.; Winnik, M. A. *J. Phys. Chem.* **1993**, *97*, 10702−10707.
(52) Yeow, E. K. L.; Ghiggino, K. P.; Reek, J. N. H.; Crossley, M. J.; Bosman, A. W.; Schenning, A. P. H. J.; Meijer, E. W. *J. Phys. Chem. B* **2000**, *104*, 2596−2606.
(53) Vuorimaa, E.; Lemmetyinen, H.; Ballet, P.; VanderAuweraer, M.; DeSchryver, F. C. *Langmuir* **1997**, *13*, 3009−3015.
(54) Levitz, P.; Drake, J. M.; Klafter, J. *J. Chem. Phys.* **1988**, *89*, 5224−5236.
(55) Lunz, M.; Bradley, A. L.; Chen, W. Y.; Gun'ko, Y. K. *J. Phys. Chem. C* **2009**, *113*, 3084−3088.
(56) Nakashima, K.; Liu, Y. S.; Zhang, P.; Duhamel, J.; Feng, J. R.; Winnik, M. A. *Langmuir* **1993**, *9*, 2825−2831.
(57) Loura, L. M. S.; Fedorov, A.; Prieto, M. *Biophys. J.* **1996**, *71*, 1823−1836.
(58) Minkowski, C.; Calzaferri, G. *Angew. Chem., Int. Ed.* **2005**, *44*, 5325−5329.
(59) Even, U.; Rademann, K.; Jortner, J.; Manor, N.; Reisfeld, R. *Phys. Rev. Lett.* **1984**, *52*, 2164−2167.
(60) Yun, C. S.; Javier, A.; Jennings, T.; Fisher, M.; Hira, S.; Peterson, S.; Hopkins, B.; Reich, N. O.; Strouse, G. F. *J. Am. Chem. Soc.* **2005**, *127*, 3115−3119.
(61) Tang, Y. Q.; He, W. H.; Lu, Y. L.; Fielden, J.; Xiang, X.; Yan, D. P. *J. Phys. Chem. C* **2014**, *118*, 25365−25373.

DOI: 10.1021/jacs.5b03071
J. Am. Chem. Soc. 2015, 137, 8161−8168